Synaptic activity bidirectionally regulates a novel sequence-specific S-Q phosphoproteome in neurons

Benjamin Siddoway[1], **Hailong Hou**[1], **Hongtian Yang**[1], **Ronald Petralia**[2], and **Houhui Xia**[1,*]

[1]Neuroscience Center, Louisiana State University Health Sciences Center, New Orleans, Louisiana, 70112

[2]National Institute on Deafness and Other Communication Disorders, NIH, Bethesda, Maryland, 20892

Abstract

Protein phosphorylation plays a critical role in neuronal transcription, translation, cell viability, and synaptic plasticity. In neurons, phospho-enzymes and specific substrates directly link glutamate release and post-synaptic depolarization to these cellular functions; however, many of these enzymes and their protein substrates remain uncharacterized or unidentified. In this article, we identify a novel, synaptically-driven neuronal phosphoproteome characterized by a specific motif of serine/threonine-glutamine ([S/T]-Q, abbreviated as SQ). These SQ-containing substrates are predominantly localized to dendrites, synapses, the soma; and activation of this SQ phosphoproteome by bicuculline application is induced via calcium influx through L-type calcium channels. On the other hand, acute application of NMDA can inactivate this SQ phosphoproteome. We demonstrate that the SQ motif kinase Ataxia-telangiectasia mutated (ATM) can also localize to dendrites and dendritic spines, in addition to other subcellular compartments, and is activated by bicuculline application. Pharmacology studies indicate that ATM and its sister kinase ATR up-regulate these neuronal SQ substrates. Phosphoproteomics identified over 150 SQ-containing substrates whose phosphorylation is bidirectionally-regulated by synaptic activity.

Keywords

Synaptic activity; Phosphorylation; SQ motif; Phosphoproteomics; L-type calcium channels

INTRODUCTION

Many neuronal functions are initiated through post-synaptic depolarization and subsequent calcium influx (Deisseroth *et al.* 2003, Zucker 1999). Protein kinases and phosphatases can link this synaptic calcium signal to diverse neuronal functions such as gene expression, cell viability, and the induction of synaptic plasticity. To this end, candidate-based approaches investigating substrates of CaMKII, CaMKIV, PP2B, and others have revealed how synaptic activity can control diverse cellular processes (Baumgartel & Mansuy 2012, Lisman *et al.* 2002, Wayman *et al.* 2008).

PI3K-like protein kinases (PIK-Ks) are identified through the homology of their catalytic domains to those of the lipid kinase family of phosphoinositol-3 kinases (PI3K). Four main protein kinases of this group have been well characterized in non-neuronal tissue and cell

*Corresponding author: Dr. Houhui Xia, Neuroscience Center of Excellence, Louisiana State University Health Sciences Center, New Orleans, Louisiana 70112, U.S.A Phone: 504-568-8524; FAX: 504-568-5801; hxia@lsuhsc.edu.

The authors declare no competing financial interests.

lines: ataxia telangiectasia mutated (ATM), ataxia telangiectasia mutated and Rad3-related (ATR), DNA-protein kinase (DNA-PK), and mammalian target of rapamycin (mTOR) (Abraham 2004). The mTOR-dependent signaling pathways are currently being extensively investigated as potential drug targets in autism and major depressive disorder (Hoeffer & Klann 2010, Jaworski & Sheng 2006); however, the remaining PIK-Ks have been significantly less well characterized in neurons. Analyses of substrates phosphorylated by ATM, ATR, and DNA-PK revealed their specific preference for serine/threonine-glutamine (S/T-Q, abbreviated as SQ) motif. Notably, while this motif is shared by ATM, ATR, and DNA-PK, the kinase mTOR does not share the SQ substrate consensus (Abraham 2004). Development of antibody against phosphorylated SQ motif has allowed for phosphoproteomic characterization of DNA damage pathways mediated by these kinases in non-neuronal cell lines (Matsuoka *et al.* 2007, Stokes *et al.* 2007). Interestingly, a recent report has discovered that both ATM and ATR can localize to neuronal cytosol and play important roles in synaptic functions in the central nervous system (Li *et al.* 2009). However, there are no in-depth neuronal substrate characterizations for these kinases.

In this article, we characterize a novel neuronal SQ phosphoproteome which localizes to the nucleus as well as cytoplasmic domains such as the neuronal soma, dendrites, and dendritic spines. These substrates are bidirectionally regulated by synaptic activity. Moreover, the activation of this SQ phosphoproteome is mediated by calcium influx from L-type calcium channels, and interestingly, acute activation of NMDA receptors can rapidly inactivate this SQ phosphoproteome. Pharmacological and immunostaining studies indicate that the ATM and ATR kinases phosphorylate at least a subset of the cytosolic neuronal SQ phosphoproteome. Finally phosphoproteomic investigation has identified over 150 SQ-containing substrates whose phosphorylation is up-regulated by synaptic activity.

Materials and Methods

Antibodies

Antibodies were obtained from Novus (Map2 MAb, mouse), Thermo-Scientific (PSD95 MAb, mouse), Santa Cruz biotechnology (B-Tubulin MAb, Mouse), Cell Signaling (pSQ MAb, Rabbit), Millipore (pS1981, Mab), Sigma (ATM MAb, Mouse), and Abcam (ATM MAb, Mouse).

Chemicals

Drugs and chemicals were purchased from Tocris Biosciences (TTX, D-AP5, CNQX, nimodipine, wortmannin, caffeine, NMDA, DHPG, W7, actinomycinD, cyclohexamide, MG132) and Sigma-Fluka (Bicuculline).

Immunofluorescence

Neurons were quickly washed with warm DPBS^{++} (Dulbecco's PBS, 1 mM CaCl$_2$, 0.5 mM MgCl$_2$, Gibco) and then fixed in 4% paraformaldehyde, 4% sucrose containing PBS solution for 20 min at room temperature (RT). Neurons were blocked and permeabilized via 4% BSA and 0.1% Triton-X100 in PBS, then subsequently incubated with primary antibody in the same blocking solution (Tris buffered solutions for phospho-antibodies) for 1 hr at RT. Neurons were then incubated with appropriate anti-mouse, anti-goat, or anti-rabbit Alexa488, 568, or 633 secondary antibodies (1:500; Molecular Probes) at RT for 1 hr. Coverslips were mounted on precleaned slides with Fluoromount G (Electron Microcopy Sciences, PA). Immunofluorescence images were viewed and captured using a Zeiss LSM 510 confocal laser scanning microscope.

Primary Neuronal Cell cultures

Primary cortical neurons were prepared from mixed sex E18 SD rat embryos. Time-pregnant SD rats were purchased from Harlan. Cells were plated at 0.5×10^6 per well in six well plates (~50k/cm^2, ~25k/cm^2 for immunostaining) on poly-L-lysine (50 μg/ml in borate buffer) coated 6 well culture dishes for biochemistry (or 24 well glass coverslips for immunostaining) in neurobasal medium supplemented with 2% B27 and 1% glutamax (Gibco), with 1 ml fresh medium per well added at DIV 2, 5 and 12, respectively. Three- to four-week old neurons were used in all experiments. All experimental protocols for live animals followed the ARRIVE guidelines (Kilkenny *et al.* 2010) and were approved by the Institutional Animal Care and Use Committee of the Louisiana State University Health Sciences Center, New Orleans.

Acute Slices

Acute brain slice cultures were prepared as described (Ascoli *et al.* 2010, Liu *et al.* 2010). Briefly, acute hippocampal slices were cut and allowed to equilibrate in ACSF for 2 hr and then treated with bicuculline or TTX. Acute cerebellar slices were cut and allowed to equilibrate for 1 hr and then treated with bicuculline in high potassium ACSF (50 mM KCL) or treated with TTX.

Immunogold Electron Microscopy (EM)

Postembedding immunogold labeling was based on established methods (Petralia *et al.* 2010). Briefly, rats were anesthetized by ketamine and xylazine before perfused with 4% paraformaldehyde plus 0.5% glutaraldehyde, and sections were cryoprotected and frozen in a Leica EM CPC (Vienna, Austria), further processed and then embedded in Lowicryl HM-20 resin using a Leica AFS freeze-substitution instrument. Thin sections were incubated in 0.1% sodium borohydride+50 mM glycine/Tris-buffered saline + 0.1% Triton X-100 (TBST), followed by 10% NGS in TBST, and primary antibody in 1% NGS/TBST overnight, and then immunogold labeling in 1% NGS in TBST plus 0.5% polyethylene glycol (20,000 MW). Finally, sections were stained with uranyl acetate and lead citrate. Corresponding controls, lacking the primary antibody, showed only rare gold labeling. Images were stored in their original formats and final images for figures were prepared in Adobe Photoshop: levels and brightness/contrast of images were minimally adjusted evenly over the entire micrograph.

Identification of Phosphorylated Proteins

Primary cortical cultures were prepared such that total cellular lysate protein concentration would exceed 20mg. These cultures were grown for 3 weeks. Half of these cultures were then treated with 40 μM bicuculline for 2 hr, and half of these cultures were then treated with 2 μM TTX for two hr. Aliquots of TTX-treated culture and bicuculline-treated culture were used to verify the responsiveness of neurons to these stimulations. Remaining treated cultures used for sequencing were then lysed in a urea-based lysis and denaturing buffer with phosphatase inhibitors. Phospho-SQ peptides were generated by trypsin digestion and purified using columns containing immobilized pSQ antibody (Cell Signaling PTM Scan group). pSQ peptides were identified by MS/MS tandem mass spectroscopy as performed previously (Stokes et al. 2007).

SQ Phosphoproteomics

Primary cortical cultures were prepared such that total cellular lysate protein concentration would exceed 20mg. Half of these cultures were then treated with 40 μM bicuculline for 2 hr, and half of these cultures were then treated with 2 μM TTX for two hr. Aliquots of TTX-treated culture and bicuculline-treated culture were used to confirm the correct

responsiveness of these neurons to TTX or bicuculline stimulations. Remaining treated cultures used for sequencing were then lysed in a urea-based lysis and denaturing buffer with phosphatase inhibitors. Phospho-SQ peptides were generated by trypsin digestion and enriched/purified using columns containing immobilized pSQ antibody (Cell Signaling PTM Scan Group). pSQ peptides were identified by MS/MS tandem mass spectroscopy as performed previously (Stokes et al. 2007). Analysis was performed on two biological replicated of TTX treatment versus bicuculline treatment in neurons (total: 4 biological samples analyzed). Phospho-peptides were subjected to reverse-phase HPLC-MS/MS, using a LTQ Orbitrap Velos mass spectrometer. We matched MS/MS spectra to R. norvegicus FASTA database using the Sorcerer-SEQUEST search engine. Supplemental figure has included Cell Signaling Technology products for total protein and site specific antibody.

Statistics

Where indicated, statistical significance was determined utilizing a two tailed student's t-test comparing control and treated samples. *p* values are listed accordingly in the accompanying figure legends.

RESULTS

Activation of a novel SQ phosphoproteome

Synaptic activity can induce signaling pathways affecting cell viability, plasticity, and morphology. In many of these studies, the drug bicuculline, a $GABA_A$ receptor antagonist, was commonly used to induce a robust increase in neuronal firing and synaptic activity. Using an antibody developed against a peptide containing phosphorylated [S/T]Q motif (termed pSQ), we determined that bicuculline-induced synaptic activation robustly induces phosphorylation of an array of neuronal SQ motif-containing substrates (Fig. 1A, B), termed the neuronal SQ phosphoproteome. Consistent with this, depolarization of neurons via incubation with extracellular high potassium isotonic solution (50 mM KCl) also induced phosphorylation of these substrates (Fig. 1C). Treatment of neurons with phosphatase inhibitor (okadaic acid) resulted in robust increases in pSQ signal, verifying that the bicuculline-induced increases observed were the result of phosphorylation of substrate proteins (Supplemental Fig. 1A). Interestingly, we found that direct activation of NMDA receptors, via treatment of cortical neurons with bath application of NMDA for 10 minutes induced robust dephosphorylation of basal SQ substrates (Fig. 1D, note: longer exposure time was used for obtaining strong basal pSQ signal). However, we found that direct activation of metabotropic glutamate receptors via DHPG bath application does not have an effect on phosphorylation of the SQ phosphoproteome (Fig. 1E). On the other hand, we observed that increases in SQ phosphorylation are not blocked by actinomycinD or cyclohexamide (Supplemental Fig. 1B, C). Moreover, bicuculline treatment has been shown by majority of reports (Ehlers 2003, Fu *et al.* 2011, Hou *et al.* 2011) to increase proteasomal degradation and our observed increase of pSQ signals due to bicuculine treatment would thus be an underestimation if pSQ proteins are degraded. Our data thus indicates that the increases of pSQ signal are a result of phosphorylation of substrate proteins but not changes in total protein level mediated via transcription, translation, or degradation, respectively (Supplemental Fig. 1B, C, D).

Localization of the SQ Phosphoproteome

Immunofluorescence (IF) studies using this antibody confirmed western blotting data that the SQ phosphoproteome is activated by bicuculline-induced activity (Fig. 2A). Moreover, IF studies revealed substantial SQ phosphoproteome signal localized outside of the nucleus (Fig. 2A, bottom panel). Visualization of these substrates along dendrites using MAP2 co-staining indicates that the cytosolic SQ phosphoproteome can localize to punctuate clusters,

morphologically consistent with dendritic spines. Co-staining with dendritic spine marker PSD-95 indicates that the dendritic SQ phosphoproteome partially localizes to synapses (Fig. 2B, C). This extra-nuclear distribution of SQ phosphoproteome is consistent with a number of recent reports that ATM/ATR can have a neuron-specific cytoplasmic localization in addition to localization in the nucleus (Borghesani *et al.* 2000, Ditch & Paull 2012, Li et al. 2009)

The SQ phosphoproteome is activated through calcium influx from L-type calcium channels

In order to investigate the signaling responsible for activation of this phosphoproteome, we focused on the immunoblot area containing the two most robustly phosphorylated substrate bands for our subsequent studies because this area shows the most robust and consistent changes (labeled as A&B in Fig. 1A. Note: bands in other immunoblot areas show similar trends in our signaling studies). Pretreatment of neurons with TTX, a sodium channel blocker that prevents action potential firing, blocked bicuculline-induced increases in SQ phosphorylation (Fig. 3A, C). This demonstrates that neuronal firing and subsequent glutamate-induced synaptic activity is necessary for the phosphorylation of SQ-containing substrates, and additionally that the SQ phosphoproteome activation is not due to a non-specific effect of bicuculline. To further delineate the receptor contributions, we pretreated neurons with AMPA receptor antagonists and/or NMDA receptor antagonists (CNQX and/ or D-AP5). When we pretreated neurons with CNQX and D-AP5 separately, we found they had no effect on activity-induced phosphorylation of SQ substrates. However, pretreatment with both drugs simultaneously (CNQX/D-AP5) blocked bicuculline-induced activation of these kinases, demonstrating that glutamate-induced post-synaptic depolarization is essential for increased SQ phosphorylation (Fig. 3A, C). Pretreatment of neurons with nimodipine, an L-type calcium channel blocker, or W7, an antagonist of Ca^{++}/calmodulin cell signaling, was sufficient to block activity-induced substrate phosphorylation (Fig. 3B, C), suggesting that membrane depolarization-induced opening of L-type calcium channels and calcium/ calmodulin dependent enzymes are essential for the phosphorylation of SQ phosphoproteome.

Inhibition of the SQ phosphoproteome

Pretreatment of neurons with a concentration of wortmannin (0.5 μM) which blocks DNA-PK and all isoforms of the PI3K and PI4K catalytic subunits does not block phosphorylation of SQ substrates (Fig. 3D). However, we found that pretreatment of neurons with wortmannin (20 μM), a concentration that inhibits PIK-K family kinases including ATM and ATR, was sufficient to block bicuculline-induced SQ phosphorylation (Fig. 3E). Moreover, pretreatment of neurons with caffeine (20 mM), another PIK-K inhibitor, was sufficient to block bicuculline-induced phosphorylation of SQ substrates (Fig. 3F). Thus, two structurally diverse inhibitors of PIK-Ks inhibit activity-induced increases in SQ substrate phosphorylation (Fig. 3E, F); indicating that PIK-Ks **may contribute to** the activation of this phosphoproteome. The relative insensitivity of these substrates to wortmannin at 0.5 μM (Fig. 3D) appears to exclude the involvement of the SQ-preferring kinase DNA-PK whose IC_{50} by wortmannin is 0.05 μM (Sarkaria *et al.* 1998).

Bidirectional regulation

We observed that treatment of neurons with TTX for 2 hours, which inhibits neuronal action potentials and thus synaptic activity, significantly reduced the phosphorylation of SQ-containing substrates identified via western blots, opposite to the results obtained from treating neurons with bicuculline (Fig. 4A). These results demonstrate that the SQ phosphoproteome is bidirectionally regulated by neuronal activity. This bidirectional

regulation of the SQ phosphoproteome was also elucidated in immunofluorescence studies; neurons treated with TTX revealed an overall decrease of pSQ signal, and a similar localization pattern as those induced by bicuculline treatment (Fig. 4B). The bidirectional regulation of the SQ phosphoproteome is not limited to primary cortical and hippocampal cultures; we also observed bi-directional SQ phosphoproteome regulation in both acute hippocampal slices (Fig. 4C) and acute cerebellar slices (Fig. 4D). different substrate bands based on molecular weight are identified in cerebellar slice preparation when compared to hippocampal slice and dissociated cortical neuron preparations, suggesting that different kinases are activated or the commonly activated kinase(s) may have different downstream targets in different brain regions.

ATM activation in response to chronic elevated neuronal activity

Our pharmacological studies have excluded PI3K, PI4K as well as DNA-PK from involvement in activity driven phosphorylation of these neuronal SQ substrates, thus leaving ATM and ATR as strong kinase candidates. Our immunofluorescence study indicates that the SQ phosphoproteome localizes to the nucleus, dendrites, as well as dendritic spines. This is consistent with reports that both ATM and ATR can localize to nucleus and cytoplasmic domains in neurons and neuron-like cell types (Boehrs *et al.* 2007, Li et al. 2009). We have confirmed and extended ATM dendritic and synapse localization in both ATM immunofluorescence and immunogold electron micrograph (EM) studies (Fig. 5 part I, II). We next asked whether ATM can be activated by bicuculline application. We determined the phosphorylation status of ATM at serine 1981, an auto-phosphorylation site on ATM and hence a marker for ATM activation. As shown in Fig. 5 part III, bicuculline treatment of cortical neurons led to increased ATM pS1981 signal in cell body as well as in proximal dendritic areas.

Phosphoproteomic analysis of the SQ phosphoproteome

Our studies so far revealed that the neuronal SQ phosphoproteome is bidirectionally regulated by synaptic activity. In order to identify the proteins in the SQ phosphoproteome, we performed a mass spectroscopy proteomic study based on immunoaffinity that has been previously utilized to identify SQ-containing substrates induced by DNA damage (Matsuoka et al. 2007, Stokes et al. 2007). Proteins in neuronal cultures, treated with TTX or bicuculline, were digested by trypsin and phospho-SQ motif-containing peptides were isolated and identified by combined pSQ antibody and liquid chromatography–tandem mass spectrometry (LC-MS/MS). The analysis yielded 244 bidirectionally regulated SQ/TQ phosphorylation sites on 150 proteins. Nearly all (232, 95%) of these sites appear to represent novel neuronal substrates, as comparison with a similar study of the SQ phosphoproteome in non-neuronal cells reveals very limited overlap (12 sites, 5%).

Identification of phospho-SQ peptides revealed 150 different SQ substrates whose phosphorylation is regulated by activity bidirectionally. Many of these proteins can localize to cytoplasm, dendrites and synapses (Fig. 6), consistent with immunofluorescence localization studies of the phosphoproteome (Fig. 2). These substrates are involved in diverse cellular processes, including G-protein receptor signaling, cell adhesion, vesicular trafficking, and scaffolding proteins, among others (Fig. 6). The detailed list of identified phospho-SQ sites, corresponding peptides, as well as the fold of phospho-SQ increase in response to bicuculline treatment, relative to TTX treatment, is provided in the supplement.

DISCUSSION

Several novel findings are discussed in this article. Our principle result is that synaptic activity drives phosphorylation of a novel neuronal SQ phosphoproteome which localizes in

the nucleus as well as in dendrites and synapses. This SQ phosphoproteome can be activated by chronic elevation of neuronal activity via L-type calcium channel mediated calcium influx. The basal SQ phosphoproteome can be suppressed by chronic inactivity in neurons and acutely inactivated by direct NMDA receptor activation. Finally we showed that ATM and perhaps ATR contribute to the phosphorylation of the SQ phosphoproteome in both cytosol and nucleus.

While many essential neuronal functions are mediated through NMDA receptors, our study elucidates a phosphoproteome-activation pathway independent of calcium influx from NMDA receptors. This likely excludes the activation of SQ substrates from a role in NMDA receptor-dependent events such as LTP and lipid modulation via the expression of COX-2, whose induction by synaptic NMDA receptor activation can be blocked by NMDA receptor antagonists (Malenka & Nicoll 1999, Stark & Bazan 2011). On the other hand, dephosphorylation of these substrates may be an important component in the induction of chemical long term depression (chemLTD) induced via bath NMDA treatment.

In non-neuronal cells, ATM/ATR mainly localize in the nucleus, performing DNA damage response functions. However, both ATM and ATR have been found to localize to cytoplasm in a neuronal-phenotypic manner (Boehrs et al. 2007, Li et al. 2009). In support of this, ATM has been found to interact with neuronal vesicular proteins VAMP, synapsin I (Li et al. 2009) and a neuronal specific isoform of beta-adaptin (Lim *et al.* 1998). Consistent with this view, we have found that ATM can localize to dendrites and synapses and further that activated ATM and pSQ phosphoproteome partially overlap in cytoplasm.

It is known that [S/T]Q is the canonical target sequence for ATM/ATR and other PIK-K kinases. Previous mass-spectrometry studies of DNA damage response pathways indicate that ATM phosphorylates many SQ-motif containing substrates (Stokes et al. 2007). Interestingly, while ATM appears to be localized inside and outside of the nucleus in neurons, DNA damaging chemicals only appear to facilitate activation of ATM within nuclear domains (Li et al. 2009, Tian *et al.* 2009). In our study we show that elevated synaptic activity appears to induce cytosolic ATM activation, but how ATM is activated is not clear. One possibility is that calcium could regulate ATM activity via regulating the activity of CDK5 (Wei *et al.* 2005) which has been reported to phosphorylate and regulate ATM activity on a site required for ATM auto-phosphorylation at S1981 (Tian et al. 2009). Future studies are needed to further elucidate the potential role of CDK5 in the SQ phosphoproteome.

Combined with pharmacology, this data suggests that ATM/ATR are the neuronal SQ kinases responsible for SQ phosphoproteome activation. However, there remain many questions. The SQ phosphoproteome can localize to dendritic spines and immunogold EM data, including dendritic spines. However, in our results, activated ATM appears to be localized dendrito-somatically. Activated synaptic ATM, although below our detection, could still be responsible for the observed strong synaptic pSQ signal, as a relatively low number of kinase enzymes may facilitate numerous substrate phosphorylations. However, it is also possible that there remain further synaptic SQ kinases which are responsible for phosphorylating the SQ substrates in spines while ATM mainly regulates SQ substrates in dendrites and cytoplasm.

Within this phosphoproteome, it is possible that ATM, ATR and other similar SQ kinases may play substantial compensatory roles. Indeed, studies investigating the PIK-K kinases have revealed multiple shared substrate proteins (Kulkarni & Das 2008, Shiloh 2003). Furthermore, kinase dead ATM knock-in mutant mice died in embryo (Daniel *et al.* 2012, Yamamoto *et al.* 2012) while other truncation ATM mutants or ATM knockout mice are

viable (Barlow *et al.* 1996, Borghesani et al. 2000, Hoeffer & Klann 2010, Xu *et al.* 1996), potentially suggesting that kinase-dead ATM may occlude essential compensatory substrate phosphorylation.

Our proteomic studies additionally provided the phospho-SQ sites and peptide/protein identity of at least of a subset of the SQ phosphoproteome. This substrate list identifies many substrates essential in neuronal functions, such as MAP2, MAP1, Cdk9, Hsp90, multiple regulators of the Rho-GTPase, the Ras GTPase (SynGap1), Synapsin-3 and translational regulatory subunits, EIF4G2 and EIF4B (Supplemental Table 2), the last of which are consistent with a potential role of the SQ phosphoproteome in gene/protein expression (van Gorp *et al.* 2009). Future studies are thus needed to validate many of these substrates and examine their roles in neuronal function, for example the role of EIF4B/G in gene expression.

In summary, our study has indicated the existence of a novel neuronal SQ phosphoproteome that is robustly and bidirectionally regulated by synaptic activity. ATM and ATR are potential kinases activating this SQ phosphoproteome which as our substrate identification suggests, play critical roles in many activity dependent neuronal functions.

Supplementary Material

Refer to Web version on PubMed Central for supplementary material.

Acknowledgments

REFERNCES

Abraham RT. PI 3-kinase related kinases: 'big' players in stress-induced signaling pathways. DNA repair. 2004; 3:883–887. [PubMed: 15279773]

Ascoli GA, Gasparini S, Medinilla V, Migliore M. Local control of postinhibitory rebound spiking in CA1 pyramidal neuron dendrites. J Neurosci. 2010; 30:6434–6442. [PubMed: 20445069]

Barlow C, Hirotsune S, Paylor R, et al. Atm-deficient mice: a paradigm of ataxia telangiectasia. Cell. 1996; 86:159–171. [PubMed: 8689683]

Baumgartel K, Mansuy IM. Neural functions of calcineurin in synaptic plasticity and memory. Learn Mem. 2012; 19:375–384. [PubMed: 22904368]

Boehrs JK, He J, Halaby MJ, Yang DQ. Constitutive expression and cytoplasmic compartmentalization of ATM protein in differentiated human neuron-like SH-SY5Y cells. Journal of neurochemistry. 2007; 100:337–345. [PubMed: 17241156]

Borghesani PR, Alt FW, Bottaro A, et al. Abnormal development of Purkinje cells and lymphocytes in Atm mutant mice. Proceedings of the National Academy of Sciences of the United States of America. 2000; 97:3336–3341. [PubMed: 10716718]

Daniel JA, Pellegrini M, Lee BS, et al. Loss of ATM kinase activity leads to embryonic lethality in mice. The Journal of cell biology. 2012; 198:295–304. [PubMed: 22869595]

Deisseroth K, Mermelstein PG, Xia H, Tsien RW. Signaling from synapse to nucleus: the logic behind the mechanisms. Curr Opin Neurobiol. 2003; 13:354–365. [PubMed: 12850221]

Ditch S, Paull TT. The ATM protein kinase and cellular redox signaling: beyond the DNA damage response. Trends Biochem Sci. 2012; 37:15–22. [PubMed: 22079189]

Ehlers MD. Activity level controls postsynaptic composition and signaling via the ubiquitin-proteasome system. Nature neuroscience. 2003; 6:231–242.

Fu AK, Hung KW, Fu WY, Shen C, Chen Y, Xia J, Lai KO, Ip NY. APC(Cdh1) mediates EphA4-dependent downregulation of AMPA receptors in homeostatic plasticity. Nature neuroscience. 2011; 14:181–189.

Hoeffer CA, Klann E. mTOR signaling: at the crossroads of plasticity, memory and disease. Trends Neurosci. 2010; 33:67–75. [PubMed: 19963289]

Hou Q, Gilbert J, Man HY. Homeostatic regulation of AMPA receptor trafficking and degradation by light-controlled single-synaptic activation. Neuron. 2011; 72:806–818. [PubMed: 22153376]

Jaworski J, Sheng M. The growing role of mTOR in neuronal development and plasticity. Mol Neurobiol. 2006; 34:205–219. [PubMed: 17308353]

Kilkenny C, Browne WJ, Cuthill IC, Emerson M, Altman DG. Improving bioscience research reporting: The ARRIVE Guidelines for Reporting Animal Research. PLoS Biol. 2010; 8:e1000412. [PubMed: 20613859]

Kulkarni A, Das KC. Differential roles of ATR and ATM in p53, Chk1, and histone H2AX phosphorylation in response to hyperoxia: ATR-dependent ATM activation. American journal of physiology. 2008; 294:L998–L1006. [PubMed: 18344416]

Li J, Han YR, Plummer MR, Herrup K. Cytoplasmic ATM in neurons modulates synaptic function. Curr Biol. 2009; 19:2091–2096. [PubMed: 19962314]

Lim DS, Kirsch DG, Canman CE, Ahn JH, Ziv Y, Newman LS, Darnell RB, Shiloh Y, Kastan MB. ATM binds to beta-adaptin in cytoplasmic vesicles. Proceedings of the National Academy of Sciences of the United States of America. 1998; 95:10146–10151. [PubMed: 9707615]

Lisman J, Schulman H, Cline H. The molecular basis of CaMKII function in synaptic and behavioural memory. Nature reviews. 2002; 3:175–190.

Liu Y, Formisano L, Savtchouk I, Takayasu Y, Szabo G, Zukin RS, Liu SJ. A single fear-inducing stimulus induces a transcription-dependent switch in synaptic AMPAR phenotype. Nature neuroscience. 2010; 13:223–231.

Malenka RC, Nicoll RA. Long-term potentiation--a decade of progress? Science (New York, NY. 1999; 285:1870–1874.

Matsuoka S, Ballif BA, Smogorzewska A, et al. ATM and ATR substrate analysis reveals extensive protein networks responsive to DNA damage. Science (New York, NY. 2007; 316:1160–1166.

Petralia RS, Wang YX, Hua F, Yi Z, Zhou A, Ge L, Stephenson FA, Wenthold RJ. Organization of NMDA receptors at extrasynaptic locations. Neuroscience. 2010; 167:68–87. [PubMed: 20096331]

Sarkaria JN, Tibbetts RS, Busby EC, Kennedy AP, Hill DE, Abraham RT. Inhibition of phosphoinositide 3-kinase related kinases by the radiosensitizing agent wortmannin. Cancer research. 1998; 58:4375–4382. [PubMed: 9766667]

Shiloh Y. ATM and related protein kinases: safeguarding genome integrity. Nat Rev Cancer. 2003; 3:155–168. [PubMed: 12612651]

Stark DT, Bazan NG. Synaptic and extrasynaptic NMDA receptors differentially modulate neuronal cyclooxygenase-2 function, lipid peroxidation, and neuroprotection. J Neurosci. 2011; 31:13710–13721. [PubMed: 21957234]

Stokes MP, Rush J, Macneill J, et al. Profiling of UV-induced ATM/ATR signaling pathways. Proceedings of the National Academy of Sciences of the United States of America. 2007; 104:19855–19860. [PubMed: 18077418]

Tian B, Yang Q, Mao Z. Phosphorylation of ATM by Cdk5 mediates DNA damage signalling and regulates neuronal death. Nature cell biology. 2009; 11:211–218.

van Gorp AG, van der Vos KE, Brenkman AB, et al. AGC kinases regulate phosphorylation and activation of eukaryotic translation initiation factor 4B. Oncogene. 2009; 28:95–106. [PubMed: 18836482]

Wayman GA, Lee YS, Tokumitsu H, Silva AJ, Soderling TR. Calmodulin-kinases: modulators of neuronal development and plasticity. Neuron. 2008; 59:914–931. [PubMed: 18817731]

Wei FY, Tomizawa K, Ohshima T, et al. Control of cyclin-dependent kinase 5 (Cdk5) activity by glutamatergic regulation of p35 stability. Journal of neurochemistry. 2005; 93:502–512. [PubMed: 15816873]

Xu Y, Ashley T, Brainerd EE, Bronson RT, Meyn MS, Baltimore D. Targeted disruption of ATM leads to growth retardation, chromosomal fragmentation during meiosis, immune defects, and thymic lymphoma. Genes Dev. 1996; 10:2411–2422. [PubMed: 8843194]

Yamamoto K, Wang Y, Jiang W, Liu X, Dubois RL, Lin CS, Ludwig T, Bakkenist CJ, Zha S. Kinase-dead ATM protein causes genomic instability and early embryonic lethality in mice. The Journal of cell biology. 2012; 198:305–313. [PubMed: 22869596]

Zucker RS. Calcium- and activity-dependent synaptic plasticity. Curr Opin Neurobiol. 1999; 9:305–313. [PubMed: 10395573]
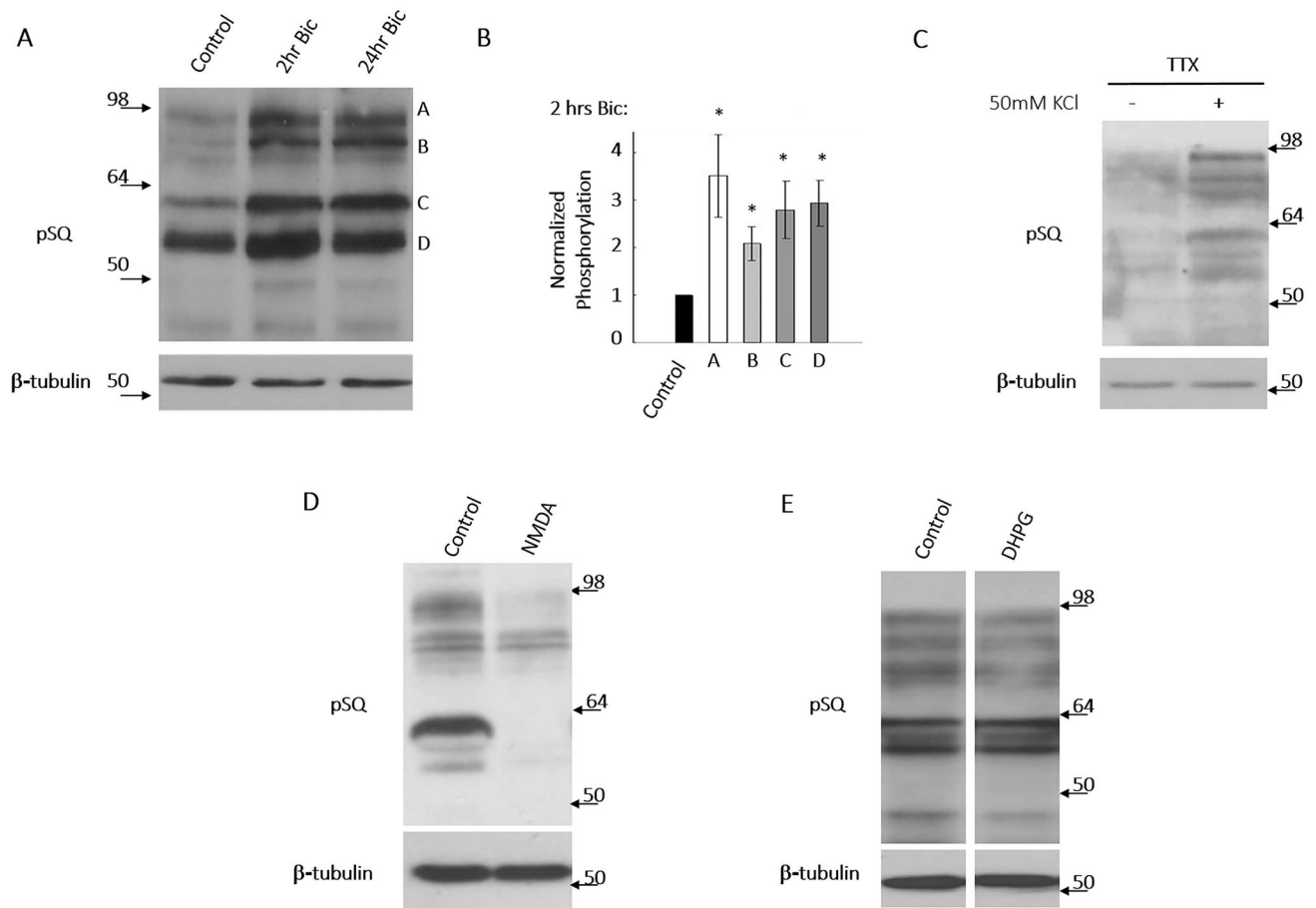
Figure 1. Synaptic activity induces activation of a SQ phosphoproteome
A & B) Treatment of neurons with 40 µM bicuculline to induce synaptic activity results in a robust increase in many bands on western blots using antibody specific to phospho-SQ motif. Bands on the blots at 2 hours bicuculline treatment time points (labeled as A, B, C and D) were quantified. Data expressed as means +/− SEM *p<0.01. C) Membrane depolarization, via incubation of neurons with isotonic 50 mM KCl ACSF solution for 15 minutes, also activates this SQ phosphoproteome. D) Acute activation of NMDA receptors, via bath application of NMDA (50 µM, 10′) shut off the basal SQ phosphoproteome (note: the exposure time for pSQ signal was extended to obtain robust basal pSQ signal). E) Direct activation of metabotropic glutamate receptors, via bath application of DHPG (50 µM, 15′), did not affect basal pSQ signal.
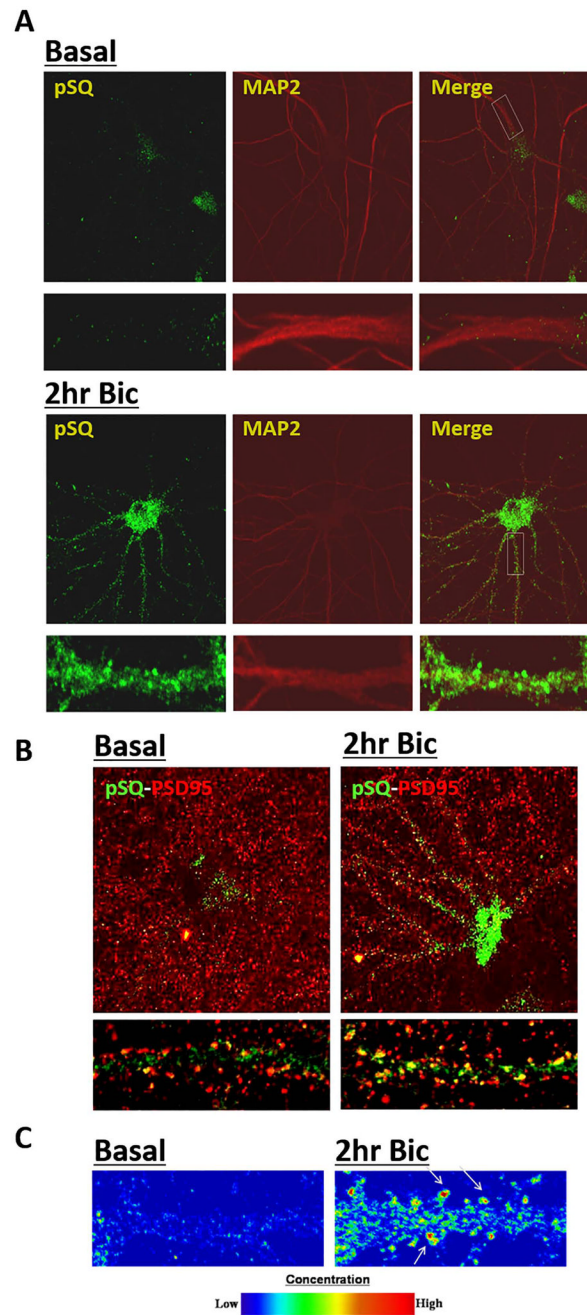
Figure 2. Localization of SQ phosphoproteome in neurons

A & B) Synaptic activity induced via 40 μM bicuculline treatment induces robust increases in phospho-SQ signals in the neuronal soma and exhibits punctate pattern along dendritic shafts (labeled by MAP2 staining in A) where it co-localizes with spine marker PSD-95 in B. C) Intensity plot of pSQ signal along dendritic processes.
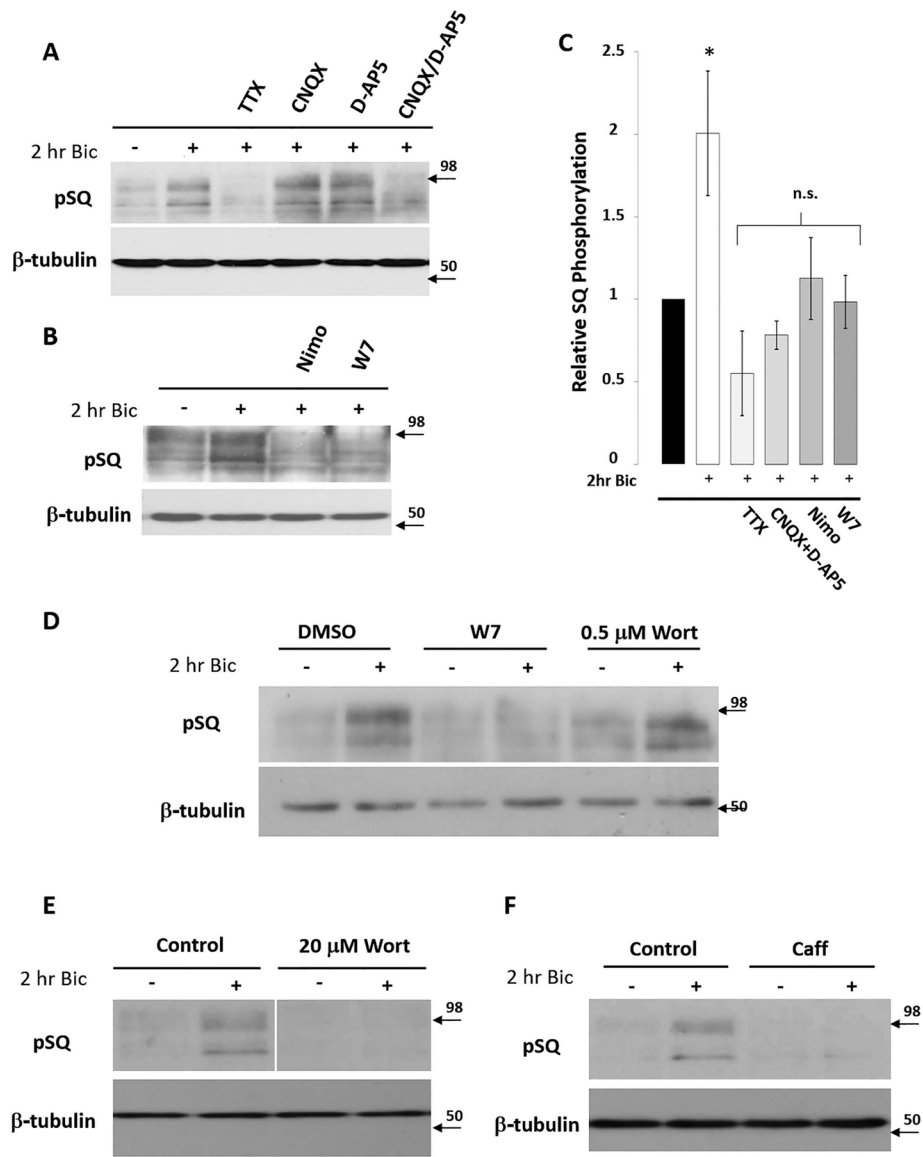
Figure 3. Pharmacological characterization of SQ phosphoproteome activation
A) Pretreatment of neurons with CNQX (40 μM), or D-AP5 (50 μM) does not block bicuculline-induced pSQ signal, while pretreatment with TTX (2 μM) or CNQX + D-AP5 does (Note: protein bands around band A&B in Fig. 1A were used for visualizing SQ phosphoproteome; bands of different molecular weights responded similarly to all pharmacological manipulations, see text). B) Pretreatment of neurons with nimodipine (Nimo: 20 μM) or W7 (25 μM) blocks the bicuculline-induced pSQ signal. C) Quantification expressed as average pixel intensity of substrate bands. Data expressed as means +/− SEM, *p<0.01. D) Pretreatment of neurons with wortmannin (Wort: 0.5 μM) did not affect bicuculline-induced pSQ signaling. Control: W7 application blocked bicuculline-induced pSQ signaling. E) Pretreatment of neurons with higher levels of wortmannin (Wort: 20 μM) blocked bicuculline-induced pSQ signaling. F) Pretreatment of neurons with caffeine (Caff: 20 mM) blocked bicuculline-induced pSQ signaling.
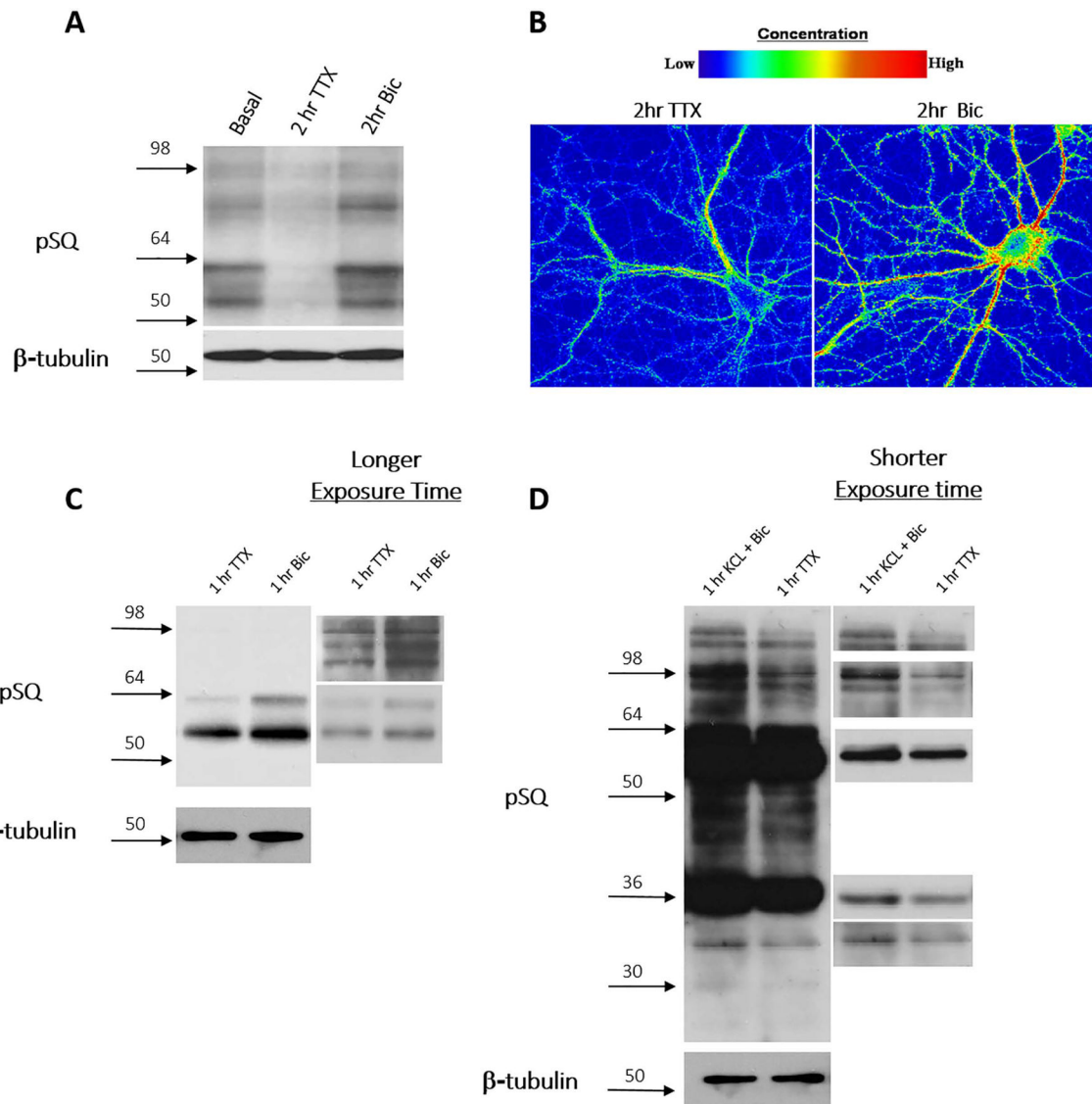
**Figure 4. The SQ phosphoproteome is bidirectionally regulated**
(A & B) TTX (2 μM for 2 hours) treatment decreases while bicuculline (40 μM, 2 hrs) treatment increases pSQ signaling in primary cortical and hippocampal neuronal cultures by western blotting (A) and confocal immunofluorescence imaging studies (B). C) Bidirectional regulation of pSQ signal in acute hippocampal slice (TTX (2μM for 1 hr) and bicuculline (40 μM for 1 hr) in ACSF). D) Bidirectional regulation of pSQ signaling in acute cerebellar slice (TTX (2 μM for 2 hours) vs. bicuculline (40μM + 50mM KCl in ACSF)).
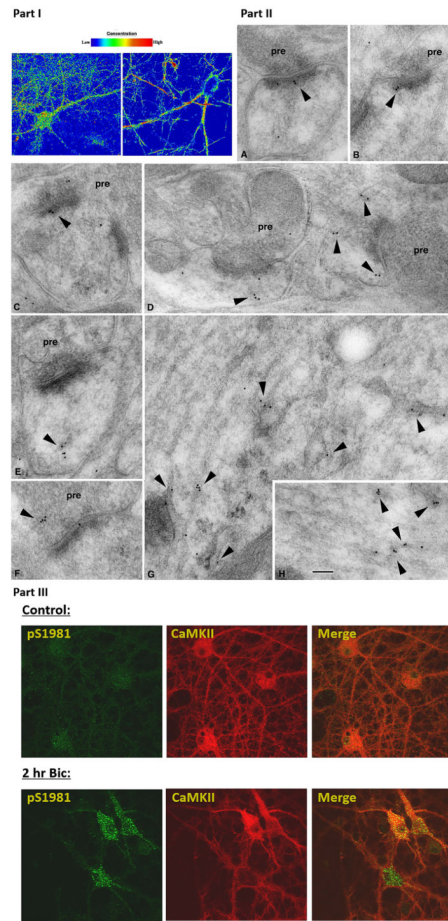
Figure 5. ATM localization and activation in neurons
Part I: Immunofluorescence localization of ATM in mixed hippocampal/cortical neurons: two different antibodies were utilized to investigate the localization of ATM in neurons (note: z-section analysis of neurons revealed substantial nuclear localization as well, see supplementary movie file). Part II: Immuno-gold electron micrograph study of ATM in the hippocampus; Labeling (arrowheads) is associated with vesicles or tubulovesicular structures in postsynaptic spines (A–E) and also in presynaptic terminals (F). In dendrites, labeling often is concentrated on tubulovesicular structures (G, H) including those associated with distinct endosomal complexes (G; straighter, regular tubular structures in G and H are microtubules running parallel to the dendrite axis). Micrographs were taken in the CA1 stratum radiatum (A, B, E, G) and pyramidale (D, H) and the CA3 stratum lucidum (C, F). pre=presynaptic terminal. Scale bar is 100 nm. Part III: ATM activation by synaptic activity. ATM pS1981, an autophosphorylation site on ATM, is determined in primary neurons treated without (control) or with (Bic) 2 hours of bicuculline. CamKII costaining indicates excitatory neurons.
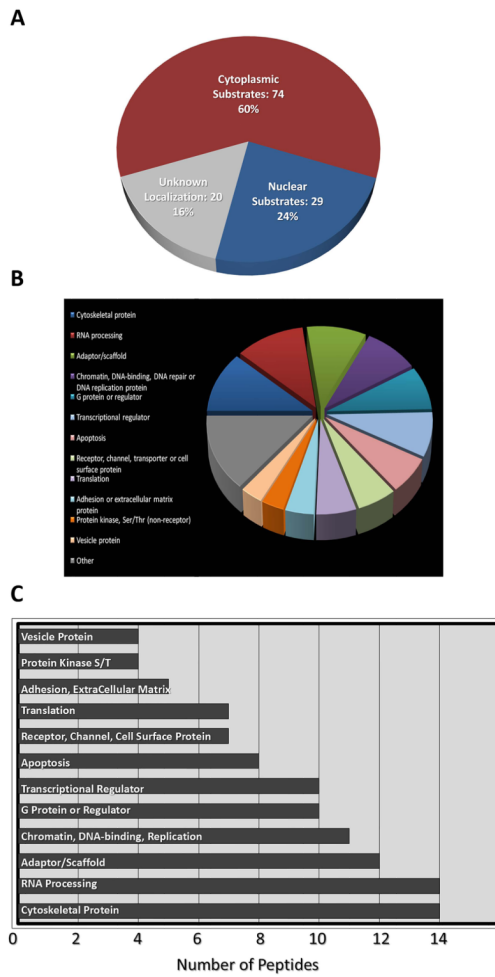
Figure 6. Identification of SQ phosphoproteome in neurons
Classification of identified peptides from phosphoproteomic identification